Degradation of Janus kinases in *CRLF2*-rearranged acute lymphoblastic leukemia

SUPPLEMENTARY INFORMATION

SUPPLEMENTARY METHODS

Abbreviations

DCM, dichloromethane; DIPEA, N,N-diisopropylethylamine; DMAP, 4-dimethylaminopyridine; DMF, dimethylformamide; DMSO, dimethyl sulfoxide; HATU, 1-[bis(dimethylamino)methylene]-1H-1,2,3-triazolo[4,5-b]pyridinium 3-oxide hexafluorophosphate; EDC, 1-ethyl-3-(3-dimehylaminopropyl)carbodiimide; NMP, N-Methyl-2-pyrrolidone; MeOH, methanol; TCFH, N,N,N',N'-tetramethylchloroformamidinium hexafluorophosphate; XPhos, 2-dicyclohexylphosphino-2′,4′,6′-triisopropylbiphenyl.

Chemistry Methods

General Methods. Chemical reagents were purchased from commercial suppliers (Ambeed, Combi-Blocks, Enamine, Oakwood, Sigma Aldrich, Strem) and were used without further purification. Thin layer chromatography was performed using Merck Millipore silica gel 60G F_{254} glass plates and visualized using a 254 nm UV lamp for detection. Microwave experiments were carried out using a Biotage Initiator system. Automated flash chromatography was performed using the Biotage SP1 flash column system with silica gel SNAP or Sfar columns. Evaporation was carried out using a Büchi Rotovapor. NMR spectra were recorded on either a Bruker 400 MHz or Bruker 500 MHz spectrometer in the solvents indicated and spectra were processed using MestReNova (12.0) referenced to the solvent peak. Purity was assessed using UPLC-MS (Acquity PDA detector, Acquity SQ detector and Acquity UPLC BEH-C18 column 1.7 µm, 2.1 x 50 mm [Waters Corp.]) with mobile phase of 0.1% formic acid in H_2O and acetonitrile. The mass spectrometer was operated in positive-ion and negative-ion modes with electrospray ionization

and data were acquired using Masslynx, version 4.1. Compounds were purified to ≥ 95% purity as assessed using LC/MS by UV/ELSD detection unless stated otherwise.

Synthesis of compound 5

Synthesis of the ester intermediate **15** was carried out by adapting a previously reported Suzuki−Miyaura coupling procedure followed by a modified Buchwald-Hartwig coupling reaction to install the pyrazole and amino benzoate moieties[1-3]. Base hydrolysis of **15** provided **16**, which was then coupled to **11** using an adapted amide coupling procedure[4] to provide **5** (Scheme 1).

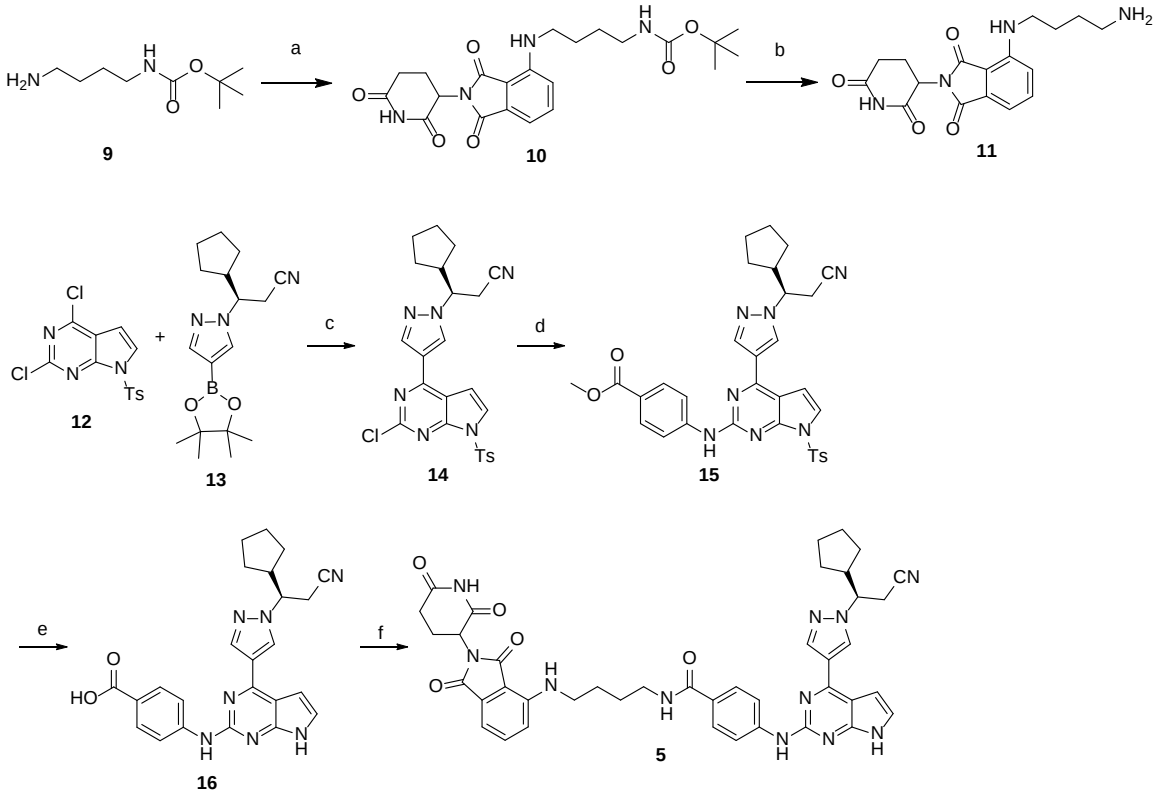

Scheme 1. Synthesis of compound **5.** Reagents and conditions: (a) 2-(2,6-dioxopiperidin-3-yl)-4-fluoroisoindoline-1,3-dione, *N*,*N*-diisopropylethylamine, dimethyl sulfoxide, 90°C, 16 h; (b) trifluoracetic acid, CH_2Cl_2, room temperature, 3 h; (c) $Pd(PPh_3)_4$, Na_2CO_3, dioxane:water (3:1), 100 °C, 1 h, 78%; (d) methyl 4-aminobenzoate, $Pd_2(dba)_3$, XPhos, K_2CO_3, *t*BuOH, 100 °C, 90

min, 90%; (e) KOH, MeOH:water (2.5:1), 75 °C, 1 h, 88%; (f) **11**, TCFH, 1-methylimidazole, MeCN, rt, 1 h, 35%.

Synthesis of compound 6

Synthesis of the ester intermediate **19** was carried out by adapting a previously reported Suzuki−Miyaura coupling procedure followed by a modified Buchwald-Hartwig coupling reaction to install the pyrazole and amino benzoate moieties[1-3]. Treating **19** briefly with base provided **3**, which was then treated with acid to provide carboxylic acid **20**. Typical amide coupling conditions between **11** and **20** provided target compound **6**.

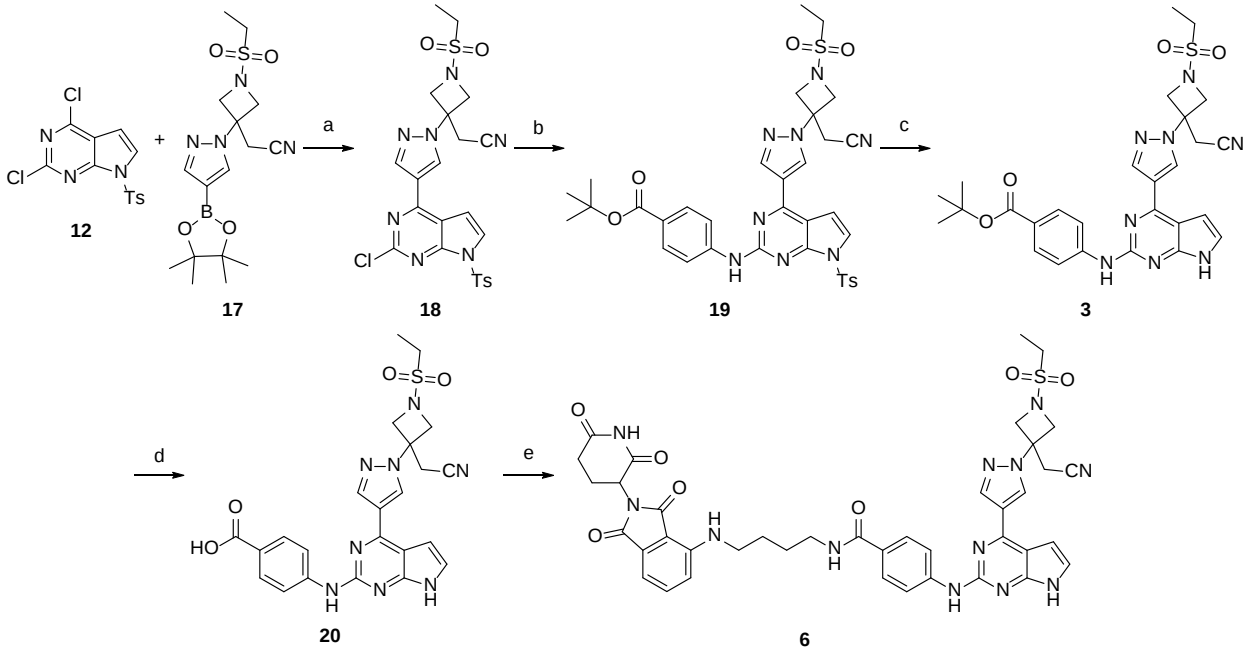

Scheme 2. Synthesis of compound **6**. Reagents and conditions: (a) $Pd(PPh_3)_4$, Na_2CO_3, dioxane:water (3:1), 100 °C, 1 h, 83%; (b) *tert*-butyl 4-aminobenzoate, $Pd_2(dba)_3$, XPhos, K_2CO_3, *t*BuOH, 100 °C, 2 h, 84%; (c) KOH, MeOH:water (2.5:1), 60 °C, 5 min, 66%; (d) DCM:TFA (1:1), rt, 1 h; (e) **11**, HATU, DIPEA, DMF, rt, 16 h, 20%.

Synthesis of compound 7

Synthesis of the ester intermediate **23** was adapted from previously reported procedures using sequential Suzuki−Miyaura and Buchwald-Hartwig coupling reactions to install the pyrazole and amino benzoate moieties[1-3]. Base hydrolysis of **23** then afforded carboxylic acid intermediate **24**. Pomalidomide linker Intermediate **11** was then coupled with **24** using typical amide coupling conditions to provide **7**. In addition, N-methyl amide analog **4** was obtained by amide coupling of carboxylic acid intermediate **24** with methylamine for X-ray crystallographic analysis with JAK2 (Scheme 3).

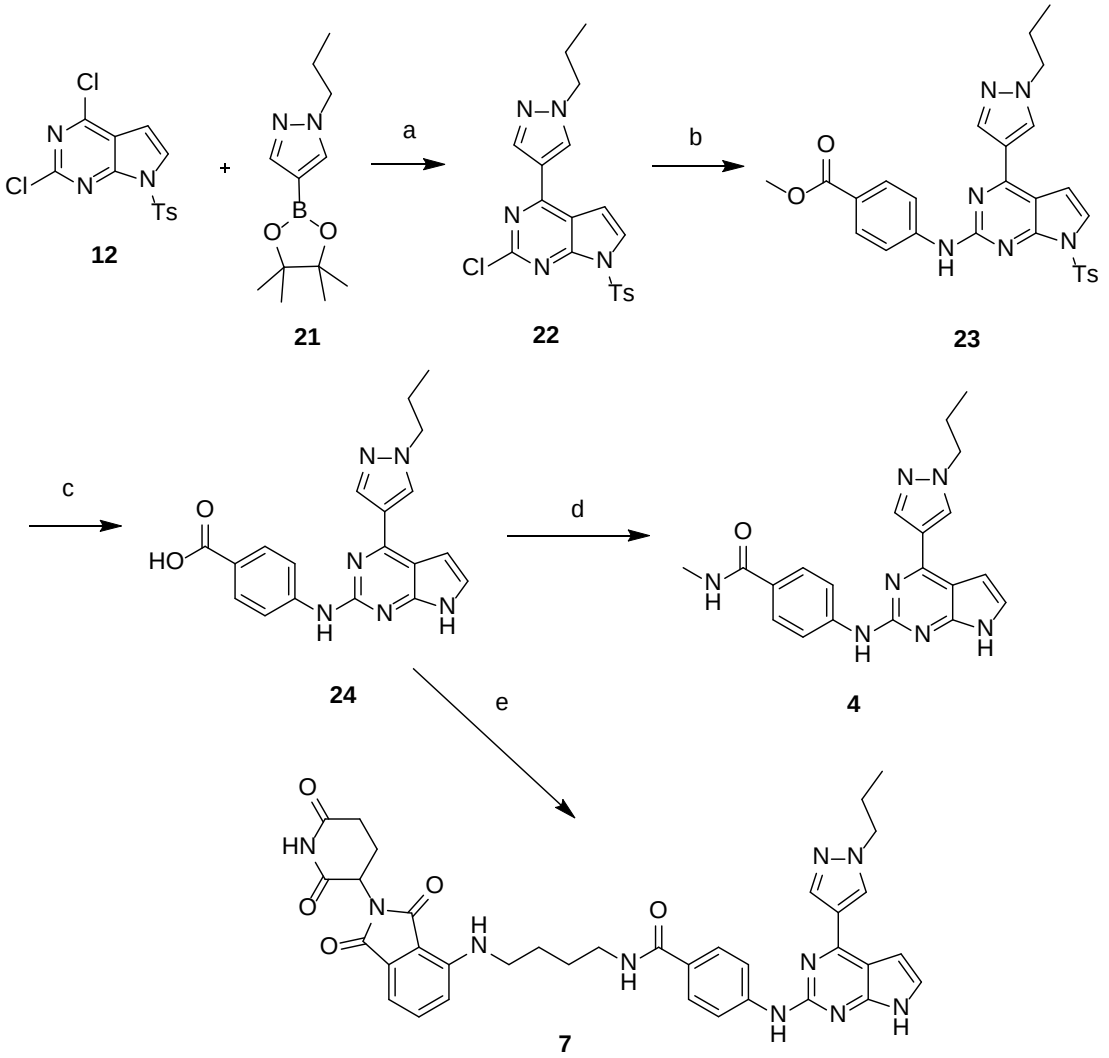

Scheme 3. Synthesis of compound **7** and **4.** Reagents and conditions (a) $Pd(Ph_3)_4$, Na_2CO_3, dioxane/water (3:1), 100°C, 2 h, 57%; (b) XPhos, $Pd_2(dba)_3$, Cs_2CO_3, dioxane, microwave, 150°C, 10 min. 78%; (c) KOH, methanol, 80°C, 2 h, 89%; (d) methylamine, HATU, *N*,*N*-diisopropylethylamine, DMF, room temperature, 3 h, 35%; (e) **20**, 1-ethyl-3-(3-dimehylaminopropyl)carbodiimide HCl, 4-dimethylaminopyridine, *N*,*N*-diisopropylethylamine, dimethylformamide, room temperature, 5 h, 41%.

Synthesis of compound 8

Intermediate **27** was prepared by nucleophilic aromatic substitution of **25** with **26.** Subsequent amine deprotection was followed by amide coupling of **28** with carboxylic acid **20** to provide **8**.

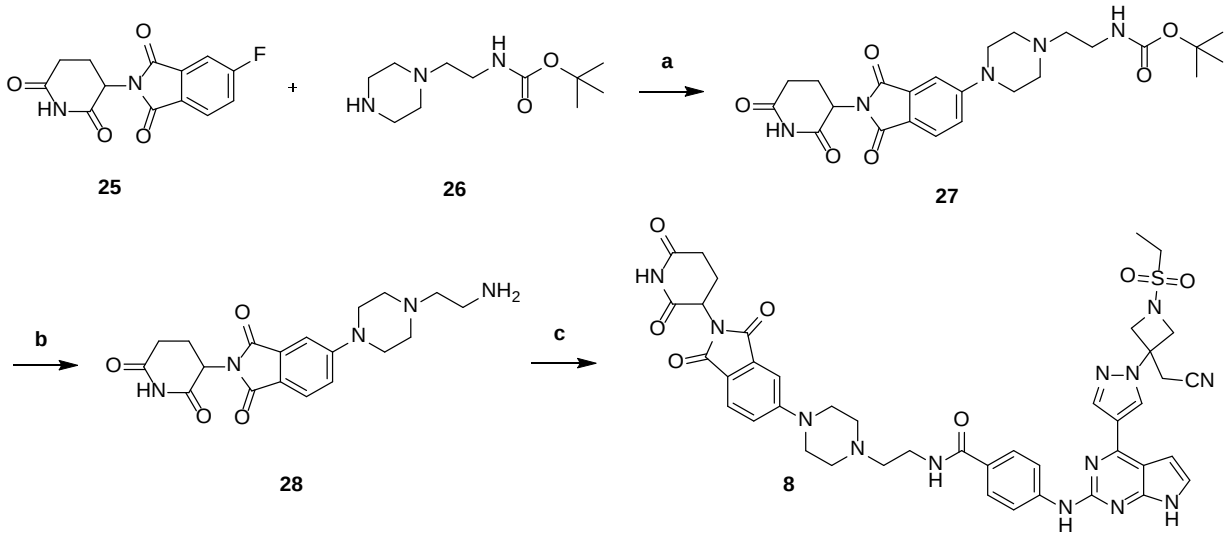

Scheme 4. Synthesis of compound **8**. Reagents and conditions: (a) *N*,*N*-diisopropylethylamine, NMP, 90°C, 16 h, 36%; (b) trifluoracetic acid, CH_2Cl_2, room temperature, 3 h; (c) carboxylic acid **20**, EDC HCl, DMAP, *N*,*N*-diisopropylethylamine, DMF, room temperature, 16 h, 17%.

Protein purification, and crystallization

Human JAK2 kinase JH1 domain (residues 835-1132, Uniprot ID O60674) was cloned into pFastBac, fused to a C-terminal His 10x tag cleavable by tobacco etch virus (TEV) protease.

Recombinant bacmid DNA containing the JAK2 insert was isolated and transfected to Spodoptera frugiperda (Sf9) insect cells to generate Baculovirus incorporated with the kinase insert. Baculovirus were amplified for two to three rounds to achieve a high titer ($2x10^8$ pfu/ml) before being used to infect BTI-Tn-5B1-4 (High Five) insect cells for protein expression. High Five insect cells were cultured in suspension to a density of 2×10^6 cells per milliliter and infected at a multiplicity of infection (MOI) greater than 10 to obtain a maximum protein yield. Infected High Five cells were incubated at 27°C for 24 hours and then at 20°C for 48 hours before harvest.

Harvested insect cell pellets were resuspended into a buffer consisting of 20 mM Tris-Cl pH 8.5, 250 mM NaCl, 0.5% Thesit, 5% glycerol, and 1 mM TECP supplemented with complete protease inhibitors cocktail (Roche), lysed by sonication, and centrifuged at 45,000g for 1 hour. The supernatant was filtered and loaded onto a Ni sepharose column (HisTrap HP, GE healthcare life sciences), and purified through nickel affinity chromatography. After extensive washes with 20 mM Imidazole supplemented suspension buffer, the His tagged protein was eluted with a linear gradient of Imidazole to 500 mM. Fractions containing JAK2 fusion protein were pooled and concentrated to 5-10 mg/ml.

The concentrated Ni column elutions were incubated with TEV protease overnight at 4°C while being dialyzed into a buffer of 20 mM Tris-Cl pH8.5, 0.25 M NaCl, 20% Glycerol, 1 mM TCEP, using 10,000 MWCO Slide-A-Lyzer dialysis cassettes (Thermo Scientific). The dialyzed sample was then diluted 10-fold in a buffer of 20 mM Tris-Cl pH 8.5, 20% Glycerol, 1 mM TCEP, before being applied to a Mono Q HR 16/60 column pre-equilibrated in 20 mM Tris-Cl pH 8.5, 25 mM NaCl, 20% Glycerol, 1 mM TCEP. Protein was eluted in a linear gradient to 500 mM NaCl. For size exclusion chromatography, Mono Q elution pool was concentrated and loaded onto Superdex 75 HiLoad 16/60 column (GE healthcare life sciences) equilibrated in 20 mM Tris-Cl pH 8, 250 mM NaCl, and 1 mM TCEP.

Crystals were grown at 18°C using the hanging drop vapor-diffusion method. The purified JAK2 kinase domain was mixed with 2 mM of the respective ligand at a concentration of 10 mg/ml and incubated at room temperature for 30 minutes, before being mixed with an equal volume of a reservoir solution. Protein-ligand complexes were co-crystalized in the three following crystallization conditions: a) 1.6-2.4 M sodium malonate, pH 5; b) 0.1 M Sodium Citrate pH 5-6.5, 21-33% polyethylene glycol 4000, 0.2 M ammonium sulfate; c) 0.1 M Sodium Citrate pH 5-6.5, 18-27% polyethylene glycol 8000, 0.2 M ammonium acetate. Crystals of all three conditions formed after 3 to 7 days.

X-ray data collection, structure determination, and refinement

Crystals were flash frozen prior to data collection using 35% glycerol or 35% ethylene glycol as cryoprotectants, supplemented in the crystallization mother liquid. Datasets of 1.5-2.5 Å resolution collected at SER-CAT beamline 22-ID (Advanced Photon Source) were merged and processed with xia2[5] in the CCP4 suite[6]. Structures were determined by the molecular replacement method using the program Phaser MR[7], using JAK2 kinase JH1 domain structure 5USY[8] as the search model. Subsequent runs of manual fitting and crystallographic refinement were performed in Coot[9], and Phenix[10]. RMSDs were calculated via SSM superposition in Coot[9]; Polder OMIT maps were calculated within Phenix[11]. Images were made with PyMOL [The PyMOL Molecular Graphics System, Version 2.0 Schrödinger, LLC.]. Interaction analysis is represented as a LigPlot+ diagram[12]. Complexes were deposited to the Protein Data Bank as 6WTN (Ruxolitinib), 6WTO (Baricitinib), 6WTP (compound **3**), and 6WTQ (compound **4**).

CRISPR-CAS9 Editing for CRBN knockdown cells

CRBN-deficient MHH-CALL-4 cell pools were generated using CRISPR-Cas9 technology. Briefly, 400,000 MHH-CALL-4 cells were transiently co-transfected with precomplexed ribonuclear proteins (RNPs) consisting of 100 pmol of chemically modified sgRNA (5' – UGUAUGUGAUGUCGGCAGAC- 3', Synthego) and 35pmol of Cas9 protein (St. Jude Protein

Production Core) via nucleofection (Lonza, 4D-Nucleofector™ X-unit) using solution P3 and program DS-150 in small (20μl) cuvettes according to the manufacturer's recommended protocol. Five days post nucleofection, a portion of cells were harvested and verified for the desired modification via targeted deep sequencing using gene specific primers with partial Illumina adapter overhangs (hCRBN.F – 5'-gcagagagtgaggaagaagatga-3' and hCRBN.R – 5'-gcccatgtcctcatccacaa-3', overhangs not shown) and analyzed using CRIS.py[13]. Sequencing analysis indicated 86% total indels and 60% out-of-frame indels for the MHH-CALL-4 edited cell pool.

In Vivo Pharmacokinetic (PK) Studies

Nontumor bearing female NSG mice (n=6), aged 8-12 weeks were dosed i.p. with single dose of compound 7 at 30 mg/kg and 100 mg/kg, respectively. Compound **7** was suspended in 60% PEG400 + 10% DMSO+10%DPBS and the dosing volume is 5ml/kg to get the target dose. For each dose, three mice were injected with a single dose and blood samples were collected at 0.5, 1, 2, 4, 8 and 24 hours by retro-orbital eye bleed technique. Blood samples (~ 0 μL) were collected and compound 7 concetration levels determined by LC-MS.

Caco-2 cell permeability

Compound Caco-2 cell permeability was measured by high throughput Caco-2 permeability assay using the Transwell® 0.4 μm polycarbonate membrane 96-well as described before[14]. Briefly, Caco-2 cells monolayers were incubated over 2 hours at 37 °C. Fractions were collected from receivers (basal side, B), and concentrations were assessed by UPLC/MS (Waters; Milford, MA). All compounds were tested in triplicates. The A→B (or B→A) apparent permeability coefficients (Papp) of each compound were calculated using the equation, Papp=dQ/dt×1/AC0, where dQ/dt equals the flux of a drug across the monolayer, A equals the total insert well surface area, and C0 is the initial concentration of substrate in the donor compartment.

KINOMEscanTM Profiling and Kd Measurement

The relative selectivity of compound **7** and **8** for Janus kinases was evaluated by KINOMEscan screening of 468 kinases at an assay concentration of 0.1μM (Eurofins DiscoveRx, San Diego, CA)[15]. TREEspot™ Kinase Dendrogram Images generated using TREEspot™ Software Tool and reprinted with permission from KINOMEscan®, a division of DiscoveRx Corporation, © DISCOVERX CORPORATION 2010. KdELECT experiments utilize the same platform that is employed for the scanMAX service with 11 dose concentration points in duplicate up to 3.0 μM.

Plasmids and Lentiviral transduction

Human full-length GSPT1 cDNA was obtained from Origene (SC327953) and G575N mutation was introduced using Q5® Site-Directed Mutagenesis Kit (New England Biolabs) using the following primers: CAA AAA ATC AAA CGA AAA AAG TAA GAC CCG AC (Forward) and TCT ACC AAG CAG ATT AAG (reverse). Then FLAG tag was added to C-terminus of both wildtype and mutant GSPT1 cDNA by PCR and cloned into ECOR I site in lentiviral vector pCL20-MSCV-IRES-GFP using the following Primers: GCG AAT TCA CCA TGG ATC CGG GCA GTG (forward) and GCG AAT TCT TAC TTA TCG TCA TCG TCT TTG TAA TCG TCT TTC TCT GGA ACC AG (reverse). The sequences of inserts were confirmed by sanger sequencing. Lentivirus pseudotyped with the BaEV-Rless (Baboon endogenous retrovirus R-less envelope protein) was generated[16] and used to transduce MHH-CALL-4 cells using RetroNectin (Takara, Cat#T100B)-coated plate in the presence of Lentiboost A and B (1:200, respectively) from SIRON Biotech. GFP expressing cells were sorted and expanded for the experiments.

Ex vivo cytotoxicity

Human CD45+ leukemic cells were purified from patient derived xenografts (PDX) by magnetic-activated cell sorting (MACS), and cytotoxicity determined by the MTT assay was then used to determine ex vivo cytotoxicity. Leukemia cells were resuspended in RPMI 1640 without

L-glutamine or phenol red (Gibco) supplemented by 10% Heat-inactivated FBS (Gibco), 2 mM L-Glutamine (Lonza), 1% Antibiotic-Antimycotic (Gibco), and 1% Insulin-Transferrin-Selenium (ITS) (Gibco) at a density of $2x10^6$ cells/mL, and 80 µL (160,000 cells) of cell suspension was then plated in round-bottom 96-well plates. Drug stocks were made by serial dilution in the cell culture medium. Duplicates were included for each of the six drug concentrations (100, 20, 4, 0.8, 0.16 and 0.032 nM for the PROTACs tested; 10000, 1000, 100, 10, 1 and 0.1 nM for CHZ868 and ruxolitinib). After 4 days incubation at 37°C/5% CO_2, 10 µL of MTT solution (ThermoFisher, dissolved in sterile 0.9% NaCl, 15mM) was added to each well. Cells were then incubated at 37°C/5% CO_2 for 4-6 hours. 100 µL of isopropanol (Sigma, supplemented with 0.04 N hydrochloric acid) was added to each well and mixed thoroughly to dissolve the Formazan crystals. The mixture was kept at room temperature for 5 minutes before measuring the absorbance at 562 nm.

Immunoblot analysis

Cells were washed twice with ice-cold PBS and lysed in RIPA lysis buffer (Sigma) freshly supplemented with Halt™ Protease Inhibitor Cocktail (ThermoFisher) for 15 minutes on ice. The cell pellet was removed by centrifugation at 13,000 g at 4°C for 15 minutes. Protein concentration was measured by BCA assay (Thermo Fisher Scientific). Proteins were denatured in NuPAGE LDS 4X sample buffer supplemented with reducing agents (Invitrogen). Typically, 10-20 µg of total protein was loaded per lane on a 4%–12% NuPAGE Bis-Tris gradient gel (Invitrogen) and analyzed by standard immunoblotting and imaged using Li-COR Odyssey CLx (LI-COR Biotechnology, Lincoln, NE). Primary antibodies used were: JAK1 (Cell Signaling #3332S), JAK2 (#3230S), JAK3 (#8827S), TYK2 (#9312S), GSPT1 (#14980S), CRBN (#71810S), IKZF1 (Santa Cruz Biotechnology, SC-398265), FLAG (Sigma, F1804) and ACBT (Santa Cruz Biotechnology, SC-47778).

Phosphoflow analysis

Cells ($7.5x10^5$) were treated with compounds in 3 ml of IMDM containing 1% BSA for one hour followed by treatment with or without 25 ng/mL TSLP (R&D systems) for 30 minutes. Cells were fixed for 10 minutes at room temperature by adding 1 ml of 10% UltraPure Formaldehyde (Polysciences), centrifuged for 5 minutes at 450g, resuspended in 95% methanol (Electron Microscopy Sciences) and store at -20°C. Cells were stained with phosphorylated (p)STAT5-Ax647(#612599, BD), pJAK2 Y1007/1008 (#3776, Cell Signaling Technologies), Anti-Rabbit-BV-421 (#406410, Biolegend), hCD45-BV605 (#564047, BD) and hCD19-PE (t#349209, BD). Mouse IgG2α-Ax647 (Cat#558053, BD) was used as isotype control. Cells were analyzed on BD Biosciences LSR/Fortessa (BD Biosciences, Franklin Lakes, NJ) with BD FACSDiva 7.0 software followed by FlowJo v10 (Tree Star, Inc., Ashland, OR).

Transcriptome analyses.

RNA-seq was performed using TruSeq stranded total library preparation and sequenced on NovaSeq sequencers (Illumina) with 100bp paired-end setting. T-ALL cell line transcriptomic data was obtained from J Cools[17]. Reads were mapped to the GRCh38 human genome reference by STAR[18] (version 2.7.1a), through the suggested two-pass mapping pipeline. Expression of genes defined by Gencode (r31) were quantified using RSEM[19] (v1.3.1). Gene fusions were detected using FusionCatcher[20]. B-ALL subtyping was performed using the in-house pipeline as detailed in Gu et al.[21] using both Prediction analysis of microarrays (PAM) and t-distributed stochastic neighbor embedding (tSNE) analysis, with the set of reference cases of known B-ALL subtypes.

Whole genome sequencing data analyses.

Xenograft samples were sequenced on NovaSeq (Illumina) with 150bp paired-end setting. Reads were mapped to human reference genome GRCh38 and mouse reference genome GRCm38 by BWA-MEM2[22] (version 2.1) separately first, and classified as human- or mouse-

specific reads or ambiguous ones using disambiguate[23]. Human-specific reads were then remapped to human reference genome GRCh38 using BWA-MEM2, and used for downstream analysis. Copy number analysis was done using Control-FREEC[24], and variant calls were generated using Mutect2[25] (GATK 4.1.8.0). Common SNPs or indels from dbSNP v150 or Gnomad exome/whole genome variants with allele frequency > 0.01 were treated as germline variants and removed. The nonsilent SNVs or indels in the known leukemia genes were manually reviewed and reported.

SUPPLEMENTARY TABLES

Supplementary Table 1. Structural data collection and refinement statistics.

Supplementary Table 2. PROTAC physicochemical properties

Supplementary Table 3. Kd of JAK PROTACs

Supplementary Table 4. Kinome scan of compound 7

Supplementary Table 5. Kinome scan of compound 8

Supplementary Table 6. Cytotoxicity of PROTACS

Supplementary Table 7. Activity of all PROTACs

Supplementary Table 8. IN vivo pharmacokinetics

Supplementary Table 9. Ex vivo cytotoxicity of patient derived xenografts

Supplementary Table 10a-c. Genomic characterization of xenografts

All tables are provided in the Supplementary Excel workbook

SUPPLEMENTARY FIGURES

Supplementary Figure 1

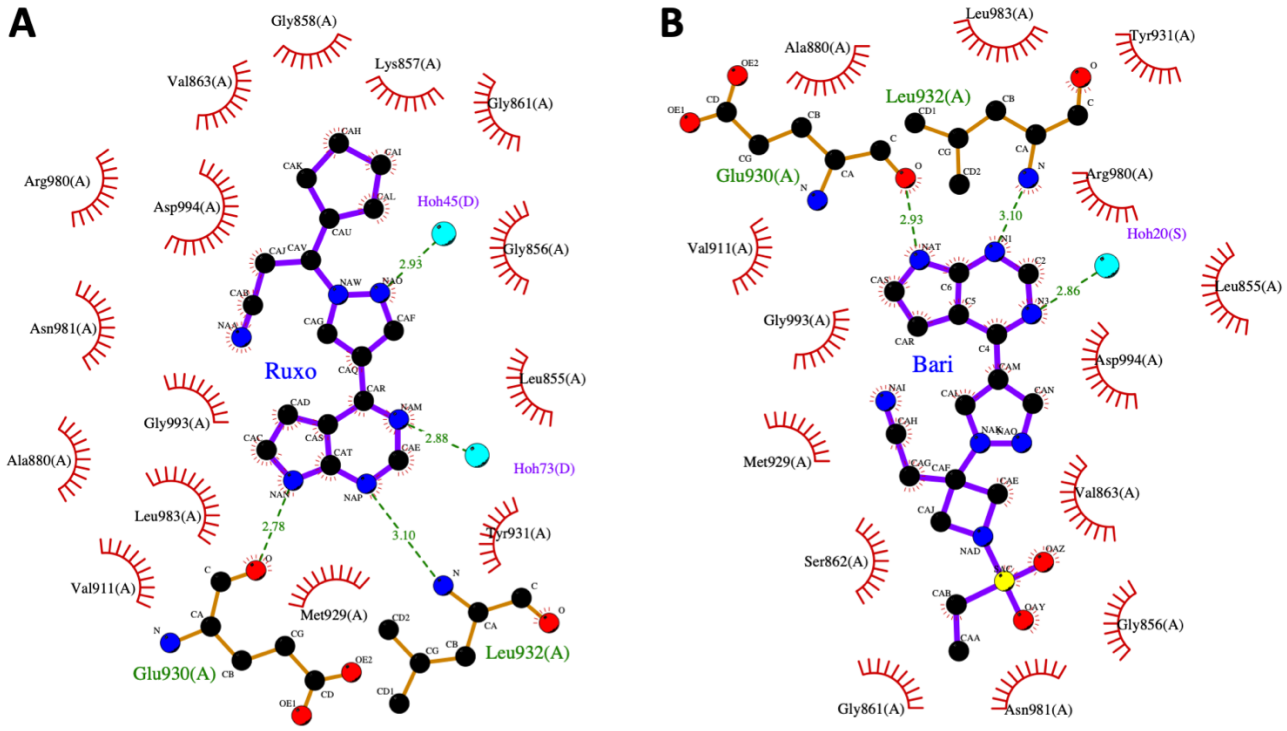

LigPlot[12] interaction analysis of ruxolitinib (**A**) and baricitinib (**B**) binding to human JAK2 JH1. Hydrogen bonds are indicated by dashed lines between the atoms involved, hydrophobic contacts are represented by an arc with spokes radiating towards the ligand atoms they contact.

Supplementary Figure 2

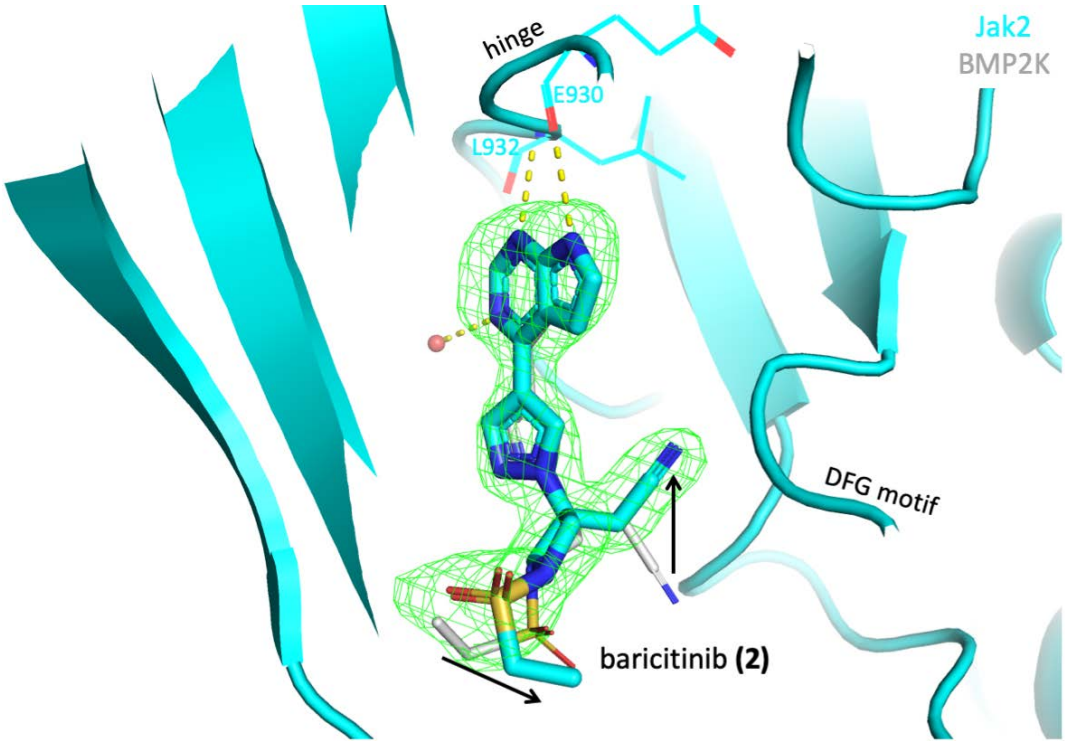

Close-up of baricitinib binding to JAK2 JH1 (cyan) displayed in **Figure 1C**; rotated to show detail of ligand changes compared to baricitinib bound to BMP2K (grey).

Supplementary Figure 3

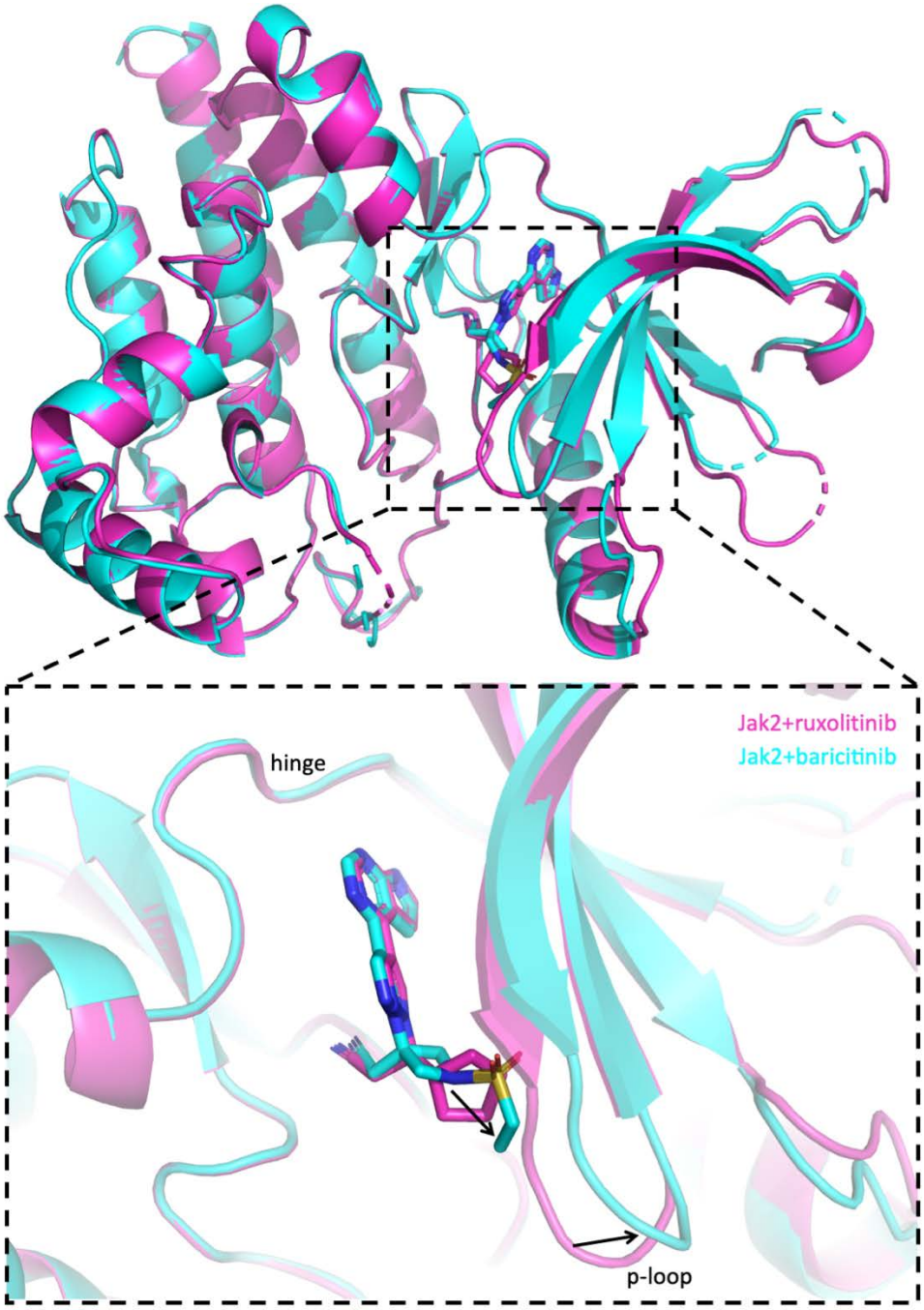

The overall structure of the JAK2 JH1 domain bound to ruxolitinib and baricitinib is very similar, both for the protein and the ligand. Ligand differences manifest in adjusted placements of the proximal p-loop to accommodate each ligand.

Supplementary Figure 4

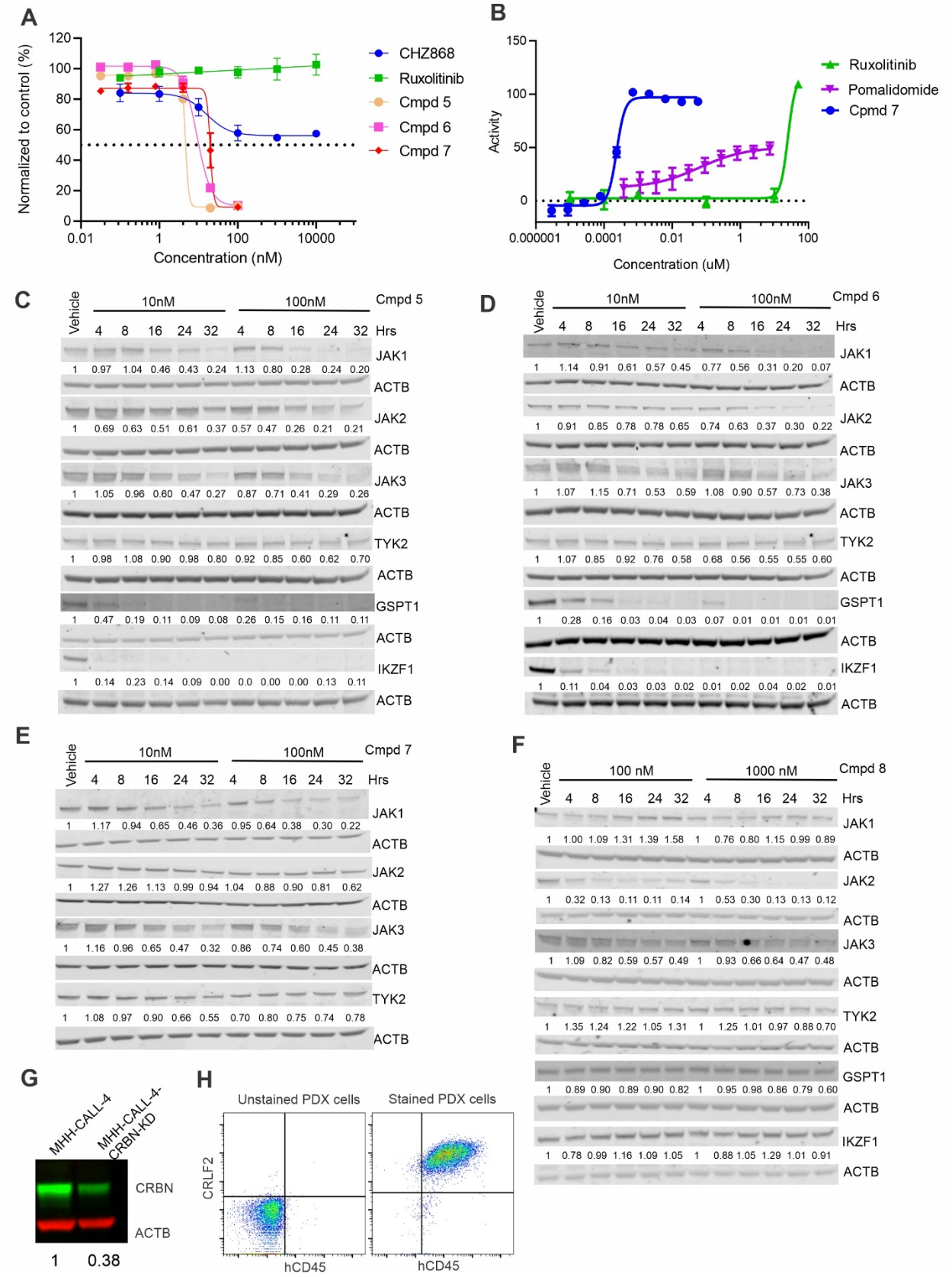

Protein degradation in MHH-CALL-4 cells treated with PROTAC compounds 5, 6 and 7. (**A**) PROTAC compounds 5, 6 and 7 but not Ruxolitinib and CHZ, two Jak2 inhibitors, show cytotoxicity in PDX cells ex vivo. (**B**) Compound 7 outcompete Ruxolitinib and pomalidomide in cytotoxicity assay in MHH-CALL-4 cells. (**C-F**) Protein degradation in MHH-CALL-4 cells at different time (up to 32 hours) treated with 10 nM and 100 nM of compounds 5 (**C**), 6 (**D**), 7 (**E**) and 8 (F). (**G**) Cereblon (CRBN) was down regulated in MHH-CALL-4-CRBN-KD cells. (**H**) Flow cytometry analysis showing overexpression of CRLF2 in hCD45+ PDX cells.

Supplementary Figure 5

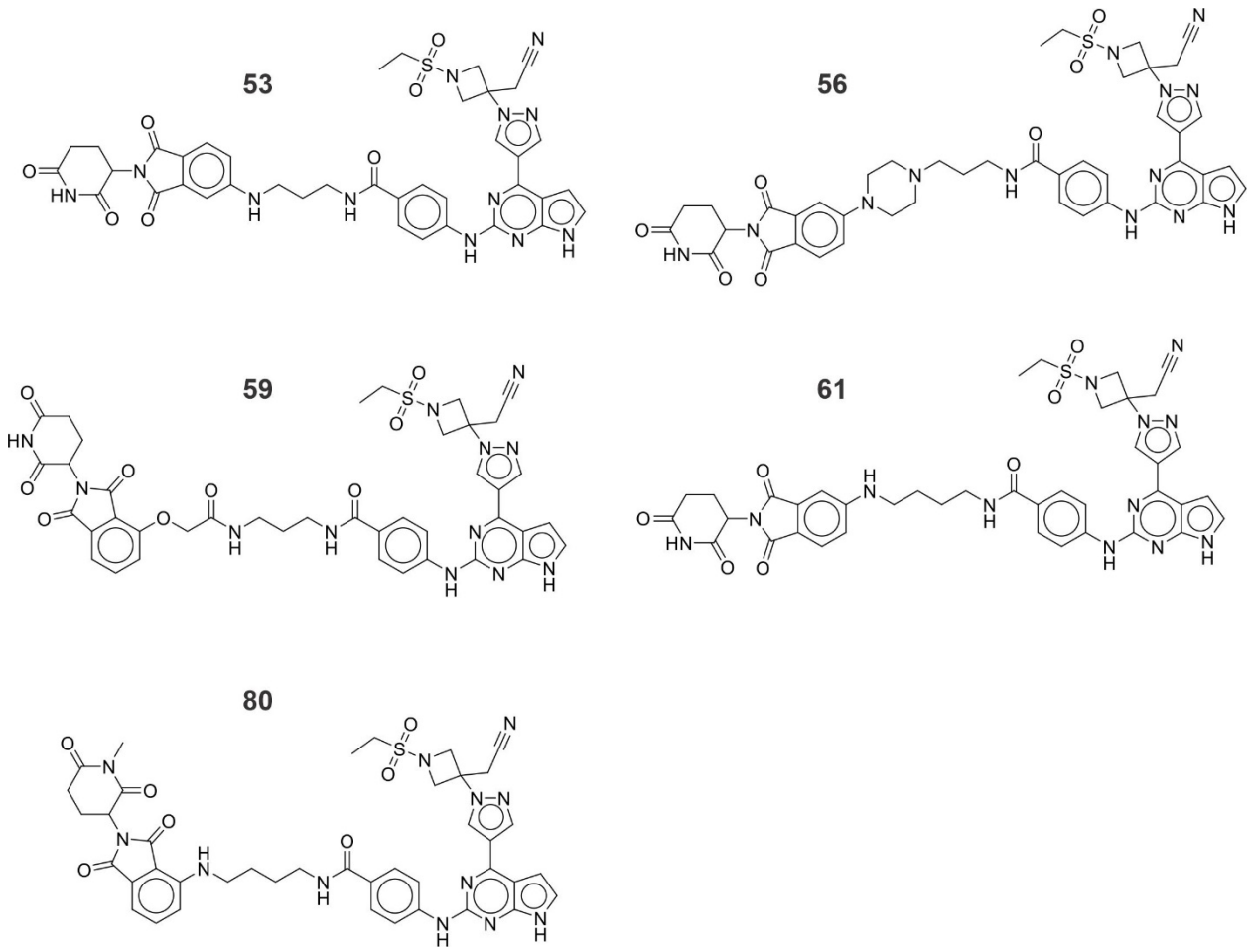

Structures of PROTACs **53**, **56**, **59**, **61** and **80** described in spider chart in Figure 3H.

Supplementary Figure 6

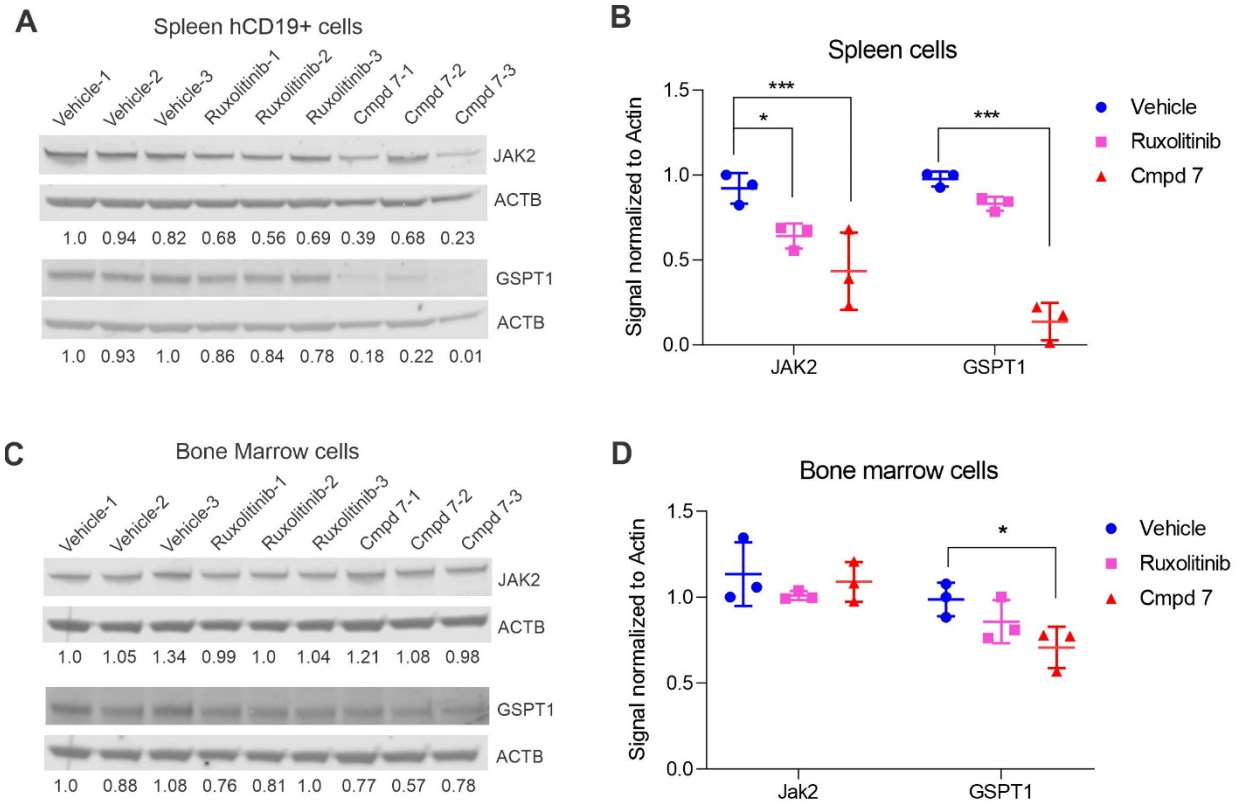

Ex vivo cytotoxicity assay of PROTAC compounds and protein degradation of compound **7** used in the in vivo efficacy study. Protein degradation of compound **7** in both spleen hCD19+ cells (**A** and **B**) and bone marrow cells (**C** and **D**) in PDX model. Quantitation of signals normalized to ACTB were shown in the graph. *P<0.05, **P<0.01, ***P<0,001 (N=3).

SUPPLEMENTARY REFERENCES

1. Yao L, Mustafa N, Tan EC, et al. Design and Synthesis of Ligand Efficient Dual Inhibitors of Janus Kinase (JAK) and Histone Deacetylase (HDAC) Based on Ruxolitinib and Vorinostat. *J Med Chem*. 2017;60(20):8336-8357.
2. Yao L, Ohlson S, Dymock BW. Design and synthesis of triple inhibitors of janus kinase (JAK), histone deacetylase (HDAC) and Heat Shock Protein 90 (HSP90). *Bioorg Med Chem Lett*. 2018;28(8):1357-1362.
3. Yao L, Ramanujulu PM, Poulsen A, Ohlson S, Dymock BW. Merging of ruxolitinib and vorinostat leads to highly potent inhibitors of JAK2 and histone deacetylase 6 (HDAC6). *Bioorg Med Chem Lett*. 2018;28(15):2636-2640.
4. Beutner GL, Young IS, Davies ML, et al. TCFH-NMI: Direct Access to N-Acyl Imidazoliums for Challenging Amide Bond Formations. *Org Lett*. 2018;20(14):4218-4222.
5. Winter G. xia2: an expert system for macromolecular crystallography data reduction. *Journal of Applied Crystallography*. 2010;43(1):186-190.
6. Winn MD, Ballard CC, Cowtan KD, et al. Overview of the CCP4 suite and current developments. *Acta Crystallographica Section D*. 2011;67(4):235-242.
7. McCoy AJ, Grosse-Kunstleve RW, Adams PD, Winn MD, Storoni LC, Read RJ. Phaser crystallographic software. *Journal of Applied Crystallography*. 2007;40(4):658-674.
8. Puleo DE, Kucera K, Hammaren HM, et al. Identification and Characterization of JAK2 Pseudokinase Domain Small Molecule Binders. *ACS Med Chem Lett*. 2017;8(6):618-621.
9. Emsley P, Lohkamp B, Scott WG, Cowtan K. Features and development of Coot. *Acta Crystallogr D Biol Crystallogr*. 2010;66(Pt 4):486-501.
10. Liebschner D, Afonine PV, Baker ML, et al. Macromolecular structure determination using X-rays, neutrons and electrons: recent developments in Phenix. *Acta Crystallogr D Struct Biol*. 2019;75(Pt 10):861-877.
11. Liebschner D, Afonine PV, Moriarty NW, et al. Polder maps: improving OMIT maps by excluding bulk solvent. *Acta Crystallographica Section D*. 2017;73(2):148-157.
12. Laskowski RA, Swindells MB. LigPlot+: multiple ligand-protein interaction diagrams for drug discovery. *J Chem Inf Model*. 2011;51(10):2778-2786.
13. Connelly JP, Pruett-Miller SM. CRIS.py: A Versatile and High-throughput Analysis Program for CRISPR-based Genome Editing. *Sci Rep*. 2019;9(1):4194.
14. Uchida M, Fukazawa T, Yamazaki Y, Hashimoto H, Miyamoto Y. A modified fast (4 day) 96-well plate Caco-2 permeability assay. *J Pharmacol Toxicol Methods*. 2009;59(1):39-43.
15. Davis MI, Hunt JP, Herrgard S, et al. Comprehensive analysis of kinase inhibitor selectivity. *Nat Biotechnol*. 2011;29(11):1046-1051.
16. Bauler M, Roberts JK, Wu CC, et al. Production of Lentiviral Vectors Using Suspension Cells Grown in Serum-free Media. *Mol Ther Methods Clin Dev*. 2020;17:58-68.
17. Atak ZK, Gianfelici V, Hulselmans G, et al. Comprehensive analysis of transcriptome variation uncovers known and novel driver events in T-cell acute lymphoblastic leukemia. *PLoS Genet*. 2013;9(12):e1003997.
18. Dobin A, Davis CA, Schlesinger F, et al. STAR: ultrafast universal RNA-seq aligner. *Bioinformatics*. 2013;29(1):15-21.
19. Li B, Dewey CN. RSEM: accurate transcript quantification from RNA-Seq data with or without a reference genome. *BMC Bioinformatics*. 2011;12:323.
20. Nicorici D, Satalan M, Edgren H, et al. FusionCatcher - a tool for finding somatic fusion genes in paired-end RNA-sequencing data. *bioRxiv*. 2014.
21. Gu Z, Churchman ML, Roberts KG, et al. PAX5-driven subtypes of B-progenitor acute lymphoblastic leukemia. *Nat Genet*. 2019;51(2):296-307.

22. Vasimuddin M, Misra S, Li H, Aluru S. Efficient Architecture-Aware Acceleration of BWA-MEM for Multicore Systems. 2019 IEEE International Parallel and Distributed Processing Symposium (IPDPS); 2019:314-324.
23. Ahdesmäki MJ, Gray SR, Johnson JH, Lai Z. Disambiguate: An open-source application for disambiguating two species in next generation sequencing data from grafted samples. *F1000Res*. 2016;5:2741.
24. Boeva V, Popova T, Bleakley K, et al. Control-FREEC: a tool for assessing copy number and allelic content using next-generation sequencing data. *Bioinformatics*. 2012;28(3):423-425.
25. DePristo MA, Banks E, Poplin R, et al. A framework for variation discovery and genotyping using next-generation DNA sequencing data. *Nat Genet*. 2011;43(5):491-498.